IEEE Access
Multidisciplinary | Rapid Review | Open Access Journal

SPECIAL SECTION ON SPECIAL SECTION ON WIRELESSLY POWERED NETWORKS
ALGORITHMS, APPLICATIONS AND TECHNOLOGIES

Received October 29, 2018, accepted November 21, 2018, date of publication December 4, 2018,
date of current version January 11, 2019.

Digital Object Identifier 10.1109/ACCESS.2018.2884916

Multi-Hop Cognitive Wireless Powered Networks: Outage Analysis and Optimization

CHI XU, (Member, IEEE), CHANGQING XIA, (Member, IEEE), CHUNHE SONG, PENG ZENG, AND HAIBIN YU, (Senior Member, IEEE)

Key Laboratory of Networked Control Systems, Shenyang Institute of Automation, Chinese Academy of Sciences, Shenyang 110016, China
Institutes for Robotics and Intelligent Manufacturing, Chinese Academy of Sciences, Shenyang 110016, China

Corresponding authors: Peng Zeng (zp@sia.cn) and Haibin Yu (yhb@sia.cn)

This work was supported in part by the National Natural Science Foundation of China under Grant 61803368 and Grant 61533015, in part by the Liaoning Provincial Natural Science Foundation of China under Grant 20180540114 and Grant 20180520029, and in part by the State Grid Corporation Science and Technology Project under Grant SG2NK00DWJS1800123.

ABSTRACT This paper analyzes and optimizes the outage performance of multi-hop cognitive wireless powered networks (CWPNs) in underlay paradigms. To be specific, there are multiple power beacons (PBs) performing wireless power transfer (WPT) for multiple battery-free secondary users (SUs). Correspondingly, the SUs first harvest energy from the RF signals of PBs and then execute multi-hop cognitive data transmission in the licensed channel concurrently with the primary users (PUs). Therefore, the transmit power of SUs are subject to the energy causality constraint imposed by WPT and the interference power constraint from multiple PUs. We derive and obtain the closed-form exact and asymptotic end-to-end outage probabilities for multi-hop CWPNs over Rayleigh block fading. Furthermore, we optimize the outage performance by studying the outage minimization problem with respect to the WPT power and the WPT time. Due to the complexity of outage probability, we propose a self-adaptive particle swarm optimization (SA-PSO)-based resource allocation algorithm to jointly optimize the power and time for WPT. Extensive simulations validate the correctness of theoretical analysis and the effectiveness of the proposed optimization algorithm.

INDEX TERMS Multi-hop, cognitive wireless powered networks, energy harvesting, outage probability, particle swarm optimization.

I. INTRODUCTION

Spectrum scarcity and energy constraint are the two most significant problems that always challenge wireless networks. To enhance spectrum utilization and energy efficiency, cognitive radio and energy harvesting technologies have been respectively investigated during the past several years. However, in cognitive radio networks (CRNs), to sufficiently protect the primary users (PUs), the secondary users (SUs) need to continually sense the channel condition and dynamically adjust their communication parameters for opportunistic spectrum access. This will surely consume a great deal of energy and aggravate the energy constraint problem. As a consequence, CRNs with energy harvesting are further investigated to simultaneously enhance spectrum utilization and energy efficiency [1].

Currently, CRNs with energy harvesting can be roughly classified into two kinds as green CRNs and cognitive wireless powered network (CWPNs). Green CRNs mainly employ renewable energy sources (e.g., solar, wind and vibration) for energy harvesting and carbon emissions reduction. However, renewable energy sources are mostly random and unstable since they are not specially designed for SUs and the energy arrivals in nature are uncertain. Therefore, renewable energy sources may not power SUs sufficiently and are usually not regarded as main energy sources, especially as SUs need to consume much energy for cognitive radio functions. In contrast, without considering renewable energy sources in nature, CWPNs employ dedicated energy sources to get on-demand energy supply. In particular, RF-based wireless power transfer (WPT) is flexible, controllable and sustainable to sufficiently power SUs. For such case, power beacons (PBs) [2] are deployed to wirelessly charge SUs, wherein the WPT parameters can be configured according to performance requirements. The recent research demonstrates that PBs with tens of Watts can power sensors, smartphones, and tablets at a distance of around 10 m [3]. It is worthy pointing out that the

RF signals of PUs are also predictable, as a result of which they are also regarded as sustainable energy sources for SUs, especially when there are excellent cooperation between PUs and SUs.

Fully considering the advantages of WPT, we investigate a multi-hop CWPN with multiple PBs underlying multiple PUs in this paper. Specifically, multiple PBs perform WPT for battery-free SUs, while SUs harvest energy from the RF signals of PBs. With the harvested energy, SUs perform multi-hop transmission in the licensed channel concurrently with multiple PUs. As such, the transmit power of SUs are constrained by the harvested energy from PBs and the peak interference power at PUs. With the formulated system model, we derive the exact end-to-end outage probability of the multi-hop CWPN over Rayleigh fading channel, and obtain the closed-form expression. Furthermore, we derive the asymptotic end-to-end outage probability to take an insight into the phenomenons when the interference power constraint is slack or strict. Based on the outage probability derivations, we further optimize the outage performance by studying an outage minimization problem in terms of the WPT power and the WPT time. Due to the complexity of outage probability and the unprovability of convexity, we propose a self-adaptive particle swarm optimization (SA-PSO)-based resource allocation algorithm to solve this problem. Simulation results validate the correctness of the theoretical analysis and the effectiveness of the proposed algorithm.

The reminder of this paper is organized as follows. Section II provides an overview on related works about CWPNs. Section III presents the system model of the underlay multi-hop CWPN with multiple PBs and multiple PUs. Section IV derives the exact and asymptotic end-to-end outage probabilities. Section V optimizes the outage performance by proposing the SA-PSO-based resource allocation algorithm to solve the outage minimization problem. Extensive simulation results are presented and analyzed in Section VI, and conclusions are drawn in Section VII.

II. RELATED WORK

According to the spectrum sharing paradigms of CRNs, there are interweave, overlay and underlay paradigms [4], which are also supported by CWPNs.

In interweave paradigms, SUs first harvest energy from the RF signals of dedicated PBs or active PUs, and then dynamically access the licensed channel when PUs are detected as inactive. [5] derives the throughput and the outage probability when SUs opportunistically harvest energy from nearby PUs. Similarly, [6] derives the spectrum access probability as well as the outage probability for cognitive device-to-device (D2D) communication, where the D2D transmitter harvests energy from both uplink and downlink channels. [7] proposes a spectrum access scheme for the throughput maximization of CWPNs, wherein SUs harvest energy from active PUs. More recently, [8] optimizes the spectrum sensing policy for CWPNs, wherein SUs harvest and transmit by utilizing the spectrum opportunities of orthogonal frequency division multiple access (OFDMA)-based PUs.

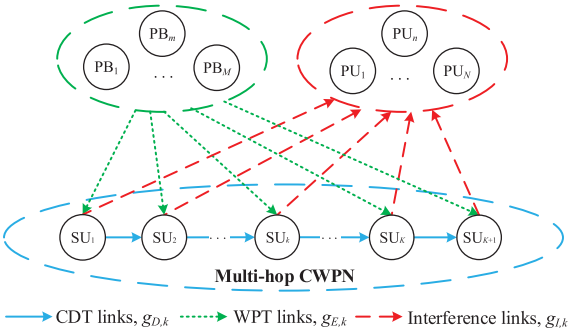

FIGURE 1. System model.

In overlay paradigms, SUs harvest energy from PBs or PUs, cooperatively transmit data for PUs and finally accomplish own data transmission missions. [9] analyzes and optimizes the outage performance of CWPNs, wherein one SU harvests energy from PU, serves as a relay for PU, and communicates with another SU. By considering multiple SUs, [10] further derives the ergodic capacity and investigates relay selection for CWPNs, wherein SUs harvest energy from PUs. [11] and [12] optimize resource allocation for sum-throughput maximization in CWPNs, wherein an access point (AP) first performs WPT for SUs as well as data transmission for PUs, and then collects data from SUs. With a similar system model, [13] further studies the energy efficiency maximization of CWPNs. More recently, [14] optimizes resource allocation for CWPNs, wherein SUs harvest energy from PUs by the power splitting scheme and transmit data for both PUs and SUs.

In underlay paradigms, SUs first harvest energy from PBs or PUs, and then transmit data under the interference power constraint from PUs, making sure that the peak interference power at PUs does not exceed a tolerable threshold. [11] studies sum-throughput maximization for CWPNs, wherein both WPT and data transmission are performed concurrently with PUs. [15] and [16] optimize resource allocation for throughput maximization in CWPNs, wherein multiple SUs harvest both energy and spectrum from one PU. [17] derives exact and asymptotic outage probabilities for the case that SUs perform simultaneous wireless information and power transfer. Our previous work [18] derives and optimizes the outage performance of multi-hop CWPNs. However, this is a special case that only one PB and one PU are considered. Thus, in this paper, we study a general case for multi-hop CWPNs with multiple PBs and multiple PUs.

III. SYSTEM MODEL

As depicted in Fig. 1, we study a multi-hop CWPN with $K+1$ battery-free SUs and M PBs underlaying N PUs. The primary base station serving PUs are assumed to be far away from SUs and do not interfere with SUs [17], [18], while PUs must be sufficiently protected such that the peak interference power at each PU is no larger than an unified threshold I_p.

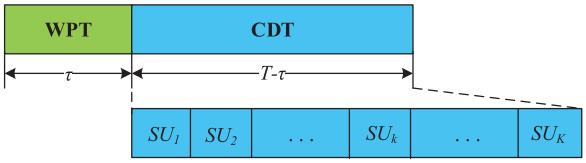

FIGURE 2. Frame structure.

There are multiple PBs located close to each other to cooperatively perform wireless power transfer (WPT) for SUs in the common channel. Meanwhile, the half-duplex SUs first harvest energy from the RF signals of PBs, and then perform cognitive data transmission (CDT) in the licensed channel within an underlay paradigm. Note that, to sufficiently power SUs and protect PUs, WPT and CDT are separated in different channels as the WPT power should be large enough in the channel with sufficient bandwidth [2]. By the time switching scheme [19], the whole communication process within one block time T is divided into two phases (i.e., WPT and CDT) as shown in Fig. 2.

In the WPT phase with duration τ $(0 < \tau < T)$, multiple PBs perform wireless power transfer while all SUs execute energy harvesting in the common channel. In this way, the harvested energy by SU_k $(k = 1, ..., K+1)$ in this phase is given by $\sum_{m=1}^{M} \xi_k \tau P_m g_{m,k}$, where P_m is the transmit power of PB_m $(m = 1, ..., M)$, $g_{m,k}$ is the channel power gain between PB_m and SU_k, $0 \le \xi_k \le 1$ is the energy harvesting efficiency. Without loss of generality, we assume that the transmit power of PBs are all equal to P_t and the energy harvesting efficiencies are all equal to ξ. Note that the noise energy is neglected since the noise power is too small to be harvested by SUs.

In the CDT phase with the remaining duration $T - \tau$, SUs execute cognitive data transmission in the licensed channel concurrently with PUs. To lower the transmit power of SUs and protect PUs, SUs perform multi-hop transmission by the time division multiple access (TDMA) mechanism. Specifically, the source SU_1 transmits data to the destination SU_{K+1} via $K-1$ immediate relaying SUs, during which decode-and-forward (DF) is utilized in each hop. For K-hop transmission, $T - \tau$ is equally divided into K timeslots, as a result of which the time for each hop transmission is $\frac{T-\tau}{K}$.

With the allocated transmission time, the maximum transmit power of SU_k constrained by its harvested energy is calculated as

$$P_{E,k} = \frac{K\xi\tau P_t \sum_{m=1}^{M} g_{m,k}}{T-\tau}, \quad k = 1, ..., K, \tag{1}$$

wherein the remaining energy before the current block is ignored since SUs are battery-free without long-time energy storage [15]. Moreover, we ignore the circuit energy consumption and assume the hardware can support the maximum transmit power achieved by WPT.

Meanwhile, to sufficiently protect PUs, the transmit power of SUs must be strictly controlled such that the peak interference power at all PUs do not exceed the prescribed interference power threshold I_p. In this way, the available transmit power of SU_k constrained by N PUs is give by

$$P_{I,k} = \frac{I_p}{\max\limits_{n=1,...,N} g_{n,k}}, \quad k = 1, ..., K, \tag{2}$$

where $g_{n,k}$ is the channel power gain between PU_n $(n = 1, ..., N)$ and SU_k, and channel reciprocity is assumed.

By fully considering the energy causality constraint imposed by WPT and the interference power constraint from multiple PUs, we can set the maximum available transmit power of SU_k as

$$P_k = \min(P_{E,k}, P_{I,k}), \quad k = 1, ..., K. \tag{3}$$

In this way, the received signal at SU_{k+1} in the licensed channel can be expressed as

$$s_{k+1} = \sqrt{P_k g_{k,k+1}} s_k + n_{k+1}, \quad k = 1, ..., K, \tag{4}$$

where $g_{k,k+1}$ is the channel power gain between SU_k and SU_{k+1}. s_k and s_{k+1} are the transmitted and the received signals of SU_k and SU_{k+1}, respectively. $n_{k+1} \sim \mathcal{CN}(0, \sigma_{k+1}^2)$ is the circularly symmetric complex Gaussian (CSCG) noise with power σ_{k+1}^2 at SU_{k+1}. For simplicity, we assume $\sigma_1^2 = ... = \sigma_{K+1}^2 = \sigma^2$.

As a consequence, the signal-to-noise ratio (SNR) for the k-th hop transmission from SU_k to SU_{k+1} is calculated as $\gamma_k = \frac{P_k g_{k,k+1}}{\sigma^2}$. More specifically, by substituting (1) and (2) into (3), we have

$$\gamma_k = \frac{\min\left(K\xi\eta P_t \sum_{m=1}^{M} g_{m,k}, \frac{I_p}{\max\limits_{n=1,...,N} g_{n,k}}\right) g_{k,k+1}}{\sigma^2}, \tag{5}$$

where $\eta = \frac{\tau}{T-\tau}$ is defined for simplicity.

In this paper, all the communication channels suffer from quasi-static block fading, namely the channel state remains constant in each block, but change independently from one to another. Meanwhile, one block fading coincides with one frame. We consider Rayleigh fading channel, where the channel power gain coefficients follow exponential distribution with rate parameter $\lambda_{X,Y}$ $(X = m, n, k; Y = k+1)$. As PBs locate close to each other, the channels from PBs to each SU follow independent identically distributed (i.i.d.). Similarly, the channels from each SU to PUs and those among SUs are also assumed to be i.i.d., respectively [20], [21]. Note that the channels among PBs, SUs and PUs are independent but not necessarily identically distributed (i.n.i.d.). As such, we denote $\lambda_{m,k} = \lambda_{E,k}$, $\lambda_{n,k} = \lambda_{I,k}$, and $\lambda_{k,k+1} = \lambda_{D,k}$ for notation convenience. Furthermore, we also assume that, at the beginning of each block, SUs and PBs can perfectly evaluate the channel state information (CSI) by channel training and estimation, pilot sensing, direct feedbacks from PUs and SUs, or even indirect feedbacks from a band manager [18].

$$P_{\text{out},k} = 1 - \frac{2}{\Gamma(M)}(\sqrt{\Delta_{1,k}})^M \mathcal{K}_M\left(2\sqrt{\Delta_{1,k}}\right) + \frac{2}{\Gamma(M)}\sum_{n=1}^{N}\binom{N}{n}(-1)^n\left((\sqrt{n\Delta_{2,k}})^M \mathcal{K}_M\left(2\sqrt{n\Delta_{2,k}}\right) - (\sqrt{\Delta_{1,k}+n\Delta_{2,k}})^M \mathcal{K}_M\left(2\sqrt{\Delta_{1,k}+n\Delta_{2,k}}\right)\right) - 2\sum_{n=1}^{N}\binom{N}{n}(-1)^n \sum_{m=0}^{M-1}\frac{n\Delta_{2,k}}{\Gamma(m+1)}\left((\sqrt{n\Delta_{2,k}})^{m-1}\mathcal{K}_{1-m}\left(2\sqrt{n\Delta_{2,k}}\right) - (\sqrt{\Delta_{1,k}+n\Delta_{2,k}})^{m-1}\mathcal{K}_{1-m}\left(2\sqrt{\Delta_{1,k}+n\Delta_{2,k}}\right)\right). \quad (7)$$

IV. OUTAGE ANALYSIS

A. EXACT OUTAGE PROBABILITY

The outage probability is defined as the probability that the instantaneous mutual information falls below a predefined threshold. For K-hop CWPN, the end-to-end outage probability P_{out} should be the probability that the throughput of the bottleneck hop is no larger than a threshold R_{th} [18]. In this way, the end-to-end outage probability can be mathematically expressed as

$$P_{\text{out}} = \Pr\left(\frac{T-\tau}{KT}\log_2(1+\min_{k=1,\ldots,K}\gamma_k) \le R_{\text{th}}\right) = 1 - \prod_{k=1}^{K}\left(1-\Pr(\gamma_k \le \gamma_{\text{th}})\right), \quad (6)$$

where $\gamma_{\text{th}} \triangleq 2^{KR_{\text{th}}(1+\eta)} - 1$ is defined as the SNR threshold. Note that $\frac{T-\tau}{KT}$ is set due to the fact that the ratio for CDT is equally divided by K for each hop transmission.

To calculate P_{out}, we must first derive the outage probability of each hop, namely $P_{\text{out},k} \triangleq \Pr(\gamma_k \le \gamma_{\text{th}})$. The following proposition gives out the closed-form expression for the outage probability of single hop.

Proposition 1: The outage probability for each hop transmission is calculated as (7), shown at the top of this page, where $\Delta_{1,k} = \frac{\lambda_{E,k}\lambda_{D,k}\gamma_{\text{th}}\sigma^2}{K\eta\xi P_t}$, $\Delta_{2,k} = \frac{\lambda_{E,k}\lambda_{I,k}I_p}{K\eta\xi P_t}$, $\Gamma(t)$ is the complete Gamma function, $\mathcal{K}_v(t)$ is the modified Bessel function of the second kind with order v.

Proof: Please refer to Appendix A for details. ■

Proposition 1 gives us the closed-form outage probability for single hop transmission. By substituting (7) into (6), we can calculate the exact end-to-end outage probability with closed-form expression. As such, for given system parameters, we can perform exact outage analysis for the multi-hop CWPN. However, the exact end-to-end outage probability is too complicated to render a clear insight into the impact of different system parameters on the outage performance. Thus, we further perform asymptotic outage analysis as follows.

B. ASYMPTOTIC OUTAGE PROBABILITY

As we can see from (5), for given channel condition and time allocation τ, the SNR significantly depends on the transmit power of PBs P_t and the peak interference power at PUs I_p. Therefore, by comparing P_t and I_p, we consider two cases to derive the asymptotic outage probabilities.

The first case is $P_t \ll I_p$ which corresponds to the scenario when the WPT power is extremely small and/or the peak interference power is extremely large. That is to say, the interference power constraint is always slack. For this case, the transmit power of SU_k is determined by its harvested energy. Hence, it is most likely to have $P_k = \min(K\xi\eta P_t\sum_{m=1}^{M} g_{m,k}, \frac{I_p}{\max_{n=1,\ldots,N} g_{n,k}}) \approx K\xi\eta P_t\sum_{m=1}^{M} g_{m,k}$. In this way, the asymptotic end-to-end outage probability with slack interference power constraint (i.e., $P_{\text{out}}^{\text{slack}}$) is calculated as the following proposition.

Proposition 2: Given τ, the asymptotic end-to-end outage probability for K-hop CWPN with slack interference power constraint (i.e., $P_t \ll I_p$) is calculated as

$$P_{\text{out}}^{\text{slack}} \overset{P_t \ll I_p}{=} 1 - \prod_{k=1}^{K}\left(\frac{2}{\Gamma(M)}(\sqrt{\Delta_{1,k}})^M \mathcal{K}_M\left(2\sqrt{\Delta_{1,k}}\right)\right). \quad (8)$$

Proof: Please refer to Appendix B for details. ■

Proposition 2 gives us the asymptotic end-to-end outage probability with slack interference power constraint. In fact, as the outage performance for this case is always determined by the harvested energy of SUs, the outage probability given by Proposition 2 is approximately equal to that of common wireless powered networks without any interference power constraint.

The second case is $P_t \gg I_p$ which corresponds to the scenario when the WPT power is extremely large and/or the peak interference power is extremely small. That is to say, the interference power constraint is always strict. For this case, I_p becomes the dominating factor for the transmit power of SU_k. Therefore, it is most likely to have $P_k = \min(K\xi\eta P_t\sum_{m=1}^{M} g_{m,k}, \frac{I_p}{\max_{n=1,\ldots,N} g_{n,k}}) \approx \frac{I_p}{\max_{n=1,\ldots,N} g_{n,k}}$. In this way, the asymptotic end-to-end outage probability with strict interference power constraint (i.e., $P_{\text{out}}^{\text{strict}}$) is given by the following proposition.

Proposition 3: Given τ, the asymptotic end-to-end outage probability for K-hop CWPN with strict interference power

constraint (i.e., $P_t \gg I_p$) is calculated as

$$P_{\text{out}}^{\text{strict}} \overset{P_t \gg I_p}{=} 1 + \prod_{k=1}^{K} \left(\sum_{n=1}^{N} \binom{N}{n} (-1)^n \frac{n\Delta_{2,k}}{\Delta_{1,k} + n\Delta_{2,k}} \right). \tag{9}$$

Proof: Please refer to Appendix C for details. ■

Proposition 3 gives us the asymptotic end-to-end outage probability with strict interference power constraint, which can be regarded as an outage floor. For this case, the outage probability would not further decrease when the WPT power attains some value. That is to say, outage saturation happens. The reason must be that SUs cannot enhance their transmit power when the interference to PUs reaches the peak interference power threshold, even the harvested energy by SUs are sufficient. In this way, the remaining energy in the battery-free SUs after transmission will be leaked. Thus, for given interference power constraint, overmuch WPT cannot significantly improve the outage performance but waste energy.

By studying the above two cases, we have a deep understanding on how the WPT parameters influence the outage performance. In the following, we further study how to set the WPT parameters properly and optimize the outage performance of multi-hop CWPNs .

V. OUTAGE OPTIMIZATION

With the closed-form end-to-end outage probability, we can observe that the outage performance of the multi-hop CWPN is determined by the channel condition and the resource allocation. As the channel condition cannot be configured, we investigate the resource allocation to optimize the outage performance. With the aim of minimizing outage probability, the resource allocation problem with respect to the WPT power and the WPT time is formulated as

$$\min_{P_t, \tau} \; P_{\text{out}}(P_t, \tau) = 1 - \prod_{k=1}^{K} \left(1 - P_{\text{out},k}(P_t, \tau)\right), \tag{10}$$

$$\text{s.t. } 0 \le P_t \le P_{\max}, \tag{11}$$

$$0 < \tau < T, \tag{12}$$

where $P_{\max}$ is the maximum transmit power of all PBs.

In this problem, the objective is to minimize the end-to-end outage probability given by (10) with (7), the constraint (11) is the WPT power constraint of PBs, and the constraint (12) is the WPT time constraint of PBs. To the best knowledge of authors, the convexity of the problem cannot be estimated due to the complex expression of the objective function. As a consequence, the outage minimization problem cannot be solved by common methods, e.g., convex optimization.

To solve the outage minimization problem, we propose a meta-heuristic algorithm based on PSO. PSO is a kind of swarm intelligent algorithm that is shown to be an effective method to achieve optimal or near-optimal solutions [23]. In comparison with other meta-heuristic algorithms, PSO, with a simple search process, is easy to implement and has a good convergence speed. The computation cost is not high when the number of optimization variables is small. Hence, it is a suitable method for our outage minimization problem.

We first model the outage minimization problem with PSO parameters. The objective function and the optimization variables correspond to the fitness and the particle position, respectively. For particle s, the outage fitness is calculated as f_s by substituting $x_{s,q}$ into (10), where $x_{s,q}$ denotes the particle position. For our problem, $q = 1$ indicates P_t and $q = 2$ indicates τ, respectively. Obviously, $x_{s,1}$ and $x_{s,2}$ must satisfy the constraints (11) and (12), respectively. Let $v_{s,q}$ denote the particle velocity, we can update it as

$$v'_{s,q} = \omega v_{s,q} + c_1\alpha(y_{s,q} - x_{s,q}) + c_2\beta(y_{g,q} - x_{s,q}), \tag{13}$$

where ω is the inertia weight, $c_1 > 0$ and $c_2 > 0$ are the learning factors, $y_{s,q}$ and $y_{g,q}$ are the local particle position and the global best particle position, respectively.

To enhance the global searching capability and avoid stopping at some local optimal positions, we further employ the self-adaptive weight alternation method to update the weight. The weight is updated as

$$\omega = \begin{cases} \omega_{\min} - \dfrac{(\omega_{\max} - \omega_{\min})(f_s - f_{\min})}{f_{\text{avg}} - f_{\min}}, & f_s \le f_{\text{avg}}, \\ \omega_{\max}, & f_s > f_{\text{avg}}, \end{cases} \tag{14}$$

where $\omega_{\min}$ and $\omega_{\max}$ are the minimum weight and the maximum weight, respectively. f_s is the current outage fitness of particle s, f_{avg} and $f_{\min}$ are the average and the minimum outage fitness of all particles, respectively.

With the self-adaptive weight alternation, we can achieve self-adaptive PSO (SA-PSO). In this way, we further propose the SA-PSO-based resource allocation algorithm to solve the outage minimization problem and optimize the resource allocation. The detail is given in Algorithm 1, where S is the number of particles, G is the maximum number of evolution iterations. In addition, κ, α, β and μ are all uniform distribution variables in $[0, 1]$. With the self-adaptive evolution of Algorithm 1, the solution will quickly coverage to the optimal or near-optimal solution, namely the best outage fitness. In this way, we can optimize the resource allocation to achieve good outage performance by Algorithm 1.

The computational complexity of Algorithm 1 can be analyzed as follows. In each evolution, the fitness of S particles is calculated. As the computational complexity for updating the particles and the velocity is much lower than that for computing the fitness, the computational complexity of Algorithm 1 mainly depends on the number of fitness computations. Let C denote the computational complexity for computing the fitness of one particle. Obviously, C is determined by the end-to-end outage probability given by (10) with (7). If the solution converges at G^* evolution, the computational complexity of Algorithm 1 can be calculated as $\mathcal{O}(CSG^*)$. As the computational complexity is a linear function of C, the computational complexity of Algorithm 1 is not high.

Algorithm 1 SA-PSO-Based Resource Allocation Algorithm

Input: $N, M, K, T, I_p, P_{\max}, \xi, \sigma^2, g_{m,k}, g_{n,k}, g_{k,k+1}$;
Output: (P_t^*, τ^*);
Initialize $s = 1$, and $t = 1$;
repeat
  Randomly generate initial particle position $x_{s,q}(t)$;
  Randomly set initial particle velocity $v_{s,q}(t)$, where $v_{s,1}(t) \in [-\kappa P_{\max}, \kappa P_{\max}]$ and $v_{s,2}(t) \in [-\kappa T, \kappa T]$;
  Calculate the outage fitness $f_s(t)$ for particle s by substituting $x_{s,q}(t)$ into (10) with (7);
  $s = s + 1$;
until $s > S$;
Record the local outage fitness $l_s(t) = f_s(t)$, where the corresponding particle position is denoted as $y_{s,q}(t) = x_{s,q}(t)$;
Calculate the global best outage fitness $g(t) = \min(l_s(t))$, where the best particle position is denoted as $y_{g,q}(t)$;
repeat
  repeat
    Update the weight ω by (14);
    Update the particle velocity as $v_{s,q}(t) = \omega v_{s,q}(t) + c_1\alpha(y_{s,q}(t) - x_{s,q}(t)) + c_2\beta(y_{g,q}(t) - x_{s,q}(t))$;
    $v_{s,1}(t) = \min(\max(-\kappa P_{\max}, v_{s,1}(t)), \kappa P_{\max})$;
    $v_{s,2}(t) = \min(\max(-\kappa T, v_{s,2}(t)), \kappa T)$;
    Update the particle position as $x_{s,q}(t) = x_{s,q}(t) + \mu v_{s,q}(t)$;
    $x_{s,1}(t) = \min(\max(0, x_{i,1}(t)), P_{\max})$;
    $x_{s,2}(t) = \min(\max(0, x_{i,2}(t)), T)$;
    Calculate the outage fitness $f_s(t)$ for particle s by substituting $x_{s,q}(t)$ into (10) with (7);
    if $f_s(t) \le l_s(t)$ **then**
      $l_s(t) = f_s(t)$ and $y_{s,q}(t) = x_{s,q}(t)$;
    if $l_s(t) \le g(t)$ **then**
      $g(t) = l_s(t)$ and $y_{g,q}(t) = y_{s,q}(t)$;
    $s = s + 1$;
  until $s > S$;
  $t = t + 1$;
until $t > G$;
$P_t^* = y_{g,1}$ and $\tau^* = y_{g,2}$;

VI. SIMULATION RESULTS

In this section, we validate the theoretical correctness of the outage probability derivations and evaluate the effectiveness of the proposed resource allocation algorithm by Monte Carlo simulations. As we consider the scenario that PBs are closely located with each other, the distances from PBs to each SU are set the same as $d_{E,k}$. One practical scenario for such simulation setups is that each PB is one antenna of an AP with multi-antenna. Similar simulation setups are also made for those from PUs to each SU as well as those among SUs, namely $d_{I,k}$ and $d_{D,k}$ [20], [21]. Then, with full consideration of the large-scale path loss, the rate parameter is calculated as

TABLE 1. Simulation parameters and values.

Description	Value
Number of hops	$K = 3$
Number of PBs	$M = 3$
Number of PUs	$N = 3$
Length of a frame	$T = 100$ ms
Maximum transmit power of PBs	$P_{\max} = 55$ dB
Peak interference power at PUs	$I_p = 10$ dB
Path loss exponent	$\varepsilon = 3$
Reference distance	$d_0 = 1$
Noise power	$\sigma^2 = 1$
Energy harvesting efficiency	$\xi = 0.8$
Outage rate threshold	$R_{\text{th}} = 1$ bps/Hz
Number of particles	$S = 50$
Maximum number of evolution iterations	$G = 100$
Learning factors	$c_1 = 1.5, c_2 = 1.5$
Inertia weight	$\omega_{\max} = 0.1, \omega_{\min} = 1.2$

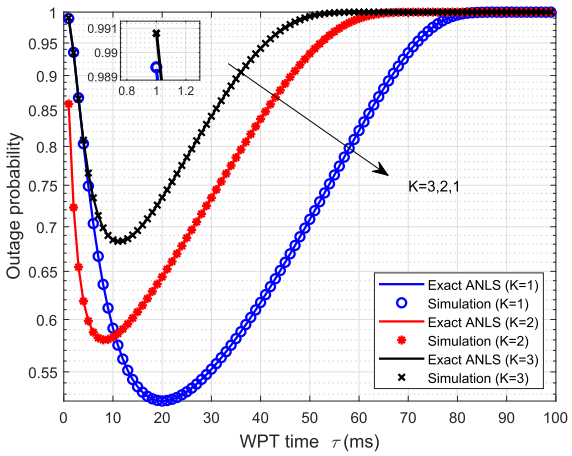

FIGURE 3. Outage probability versus WPT time for different numbers of hops: $M = 3$, $N = 3$, $I_p = 10$ dB, $P_t = 40$ dB.

$\lambda_{X,Y} = (\frac{d_{X,Y}}{d_0})^{\varepsilon}$, where d_0 is the reference distance and ε is the path loss parameter. Without loss of generality, PB_m and PU_n are placed at [0, 2] and [0, -2] on y-axis, while the source SU_1 and the destination SU_{K+1} are placed at [-2, 0] and [2, 0] on x-axis, wherein the relaying SUs are equally scattered. Unless otherwise stated, the key simulation parameters are listed in Table 1.

Fig. 3 depicts the relationship between the outage probability and the WPT time. First of all, we can observe that there is a good agreement between the theoretical analysis (ANLS) and the simulation results, which validates the correctness of theoretical derivations. Then, for each given number of hops K, the outage probability first decreases to the minimum value and then increases to 1 along with the increase of the WPT time. The reason should be that there is a tradeoff for the time allocation between WPT and CDT. In other words,

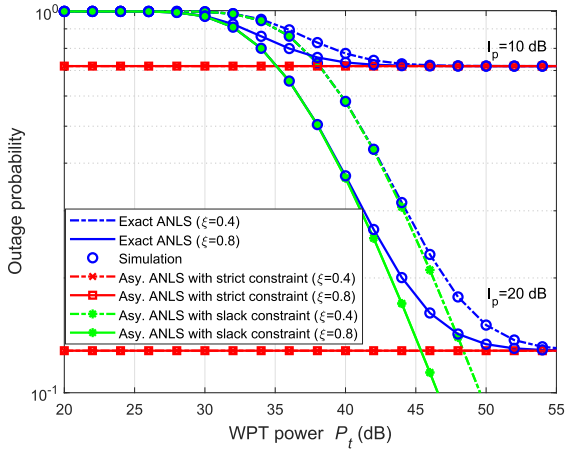

FIGURE 4. Outage probability versus WPT power for different energy harvesting efficiencies: $M = 3$, $N = 3$, $K = 3$, $\tau = 20$ ms.

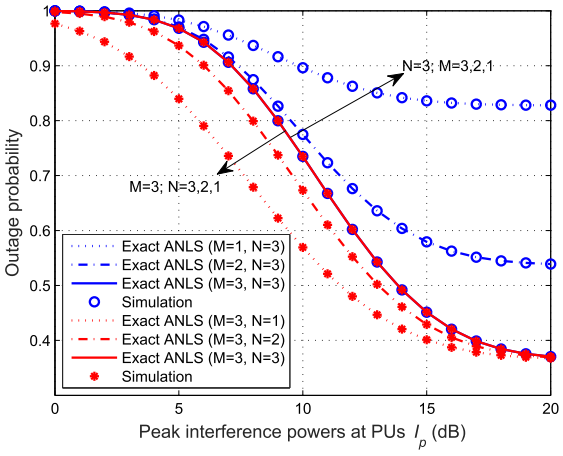

FIGURE 5. Outage probability versus peak interference power at PUs for different numbers of PUs and PBs: $K = 3$, $P_t = 40$ dB, $\tau = 20$ ms.

if more time is allocated for WPT, less time is remained for CDT, and vice versa. Meanwhile, for given WPT time τ, it is observed that there are intersections between the curves for different numbers of hops, indicating that the outage probability is not monotonic in K. Due to the complexity of the outage probability, we cannot obtain the exact expression for the optimal or near-optimal K and τ. For this case, some meta-heuristic algorithms or exhaustive searching are feasible options.

Fig. 4 studies how the WPT power impact the outage probability of a three-hop CWPN. When the WPT power is very small, the outage probability approaches 1, indicating that SUs are not effectively charged by WPT. For this case, the transmit power of SUs are mainly subject to their harvested energy. In this way, the exact outage probability approximates the asymptotic outage probability with slack constraint, which validates the correctness of Proposition 2. Then, with the increase of P_t or ξ, the outage probability monotonically decreases since SUs can harvest more energy from WPT, which surely enhances the transmit power of SUs under the interference power constraint from PUs. When the WPT power is large enough, the outage probability with the same interference power constraint converges to the same value, namely outage floor. That is to say, outage saturation happens when the WPT power is sufficient large. For this case, the transmit power of SUs are mainly subject to the interference power constraint from PUs. As such, the exact outage probability coincides with the asymptotic outage probability with strict constraint, which verifies the correctness of Proposition 3. The outage saturation phenomenon indicates that excessively large WPT power will not further enhance outage performance but waste energy.

In addition, for the same energy harvesting efficiency (e.g., $\xi = 0.8$), it is obvious that the outage probability with strict interference constraint is always higher than that with slack interference constraint. Meanwhile, the outage floor decreases when the interference power constraint becomes slack, namely I_p increases. By studying Fig. 4, we can observe that, for given system setup and channel condition, we can find the effective WPT power region according to outage requirements. However, to find the exact optimal or near-optimal P_t, we can only employ some meta-heuristic algorithms as the expression of outage probability is too complicated.

Fig. 5 further demonstrates how PUs impact the outage performance of a three-hop CWPN with different numbers of PBs. First of all, we can obverse that no matter how many PBs or PUs influence the multi-hop CWPN, the outage probability always decreases with the increase of the peak interference power. This is because SUs can enhance their transmit power with the interference power constraint releasing. However, when the peak interference power attains some value, the outage probability does not further decrease. This is because the transmit power of SUs constrained by the limited harvested energy cannot be further enhanced. Furthermore, for given number of PBs, the outage probability decreases with the number of PUs decreasing since the interference power constraint releases with N decreasing. In contrast, for given number of PUs, the outage probability increases with the number of PBs decreasing since the harvested energy by SUs decrease with M decreasing.

Fig. 6 shows the optimized outage probability by the proposed SA-PSO-based resource allocation algorithm. Although the changing trend in Fig. 6 is similar to that in Fig. 5, the outage probability is significantly decreased by the proposed algorithm. For example, when $M = N = K = 3$ and $I_p = 10$ dB, $P_{\text{out}} = 0.734$ in Fig. 5 is much larger than that $P_{\text{out}} = 0.579$ in Fig. 6. This is because the resource allocation in Fig. 5 is fixed while that in Fig. 6 is optimized according to the system setup and the channel condition. This verifies the effectiveness of the proposed algorithm. In this way, for given system setup and channel condition, we can properly configure the WPT parameters and optimize the outage performance.

Furthermore, we also compare the SA-PSO-based algorithm with the exhaustive-searching-based algorithm. It is obvious that the outage probability by the proposed

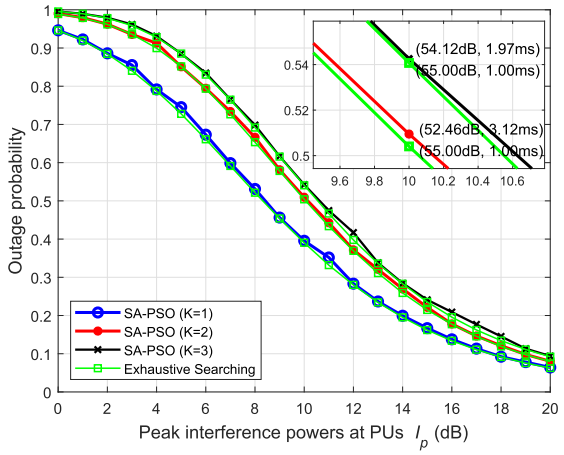

FIGURE 6. Optimized outage probability versus peak interference power at PUs for different numbers of hops: $M = 3$, $N = 3$.

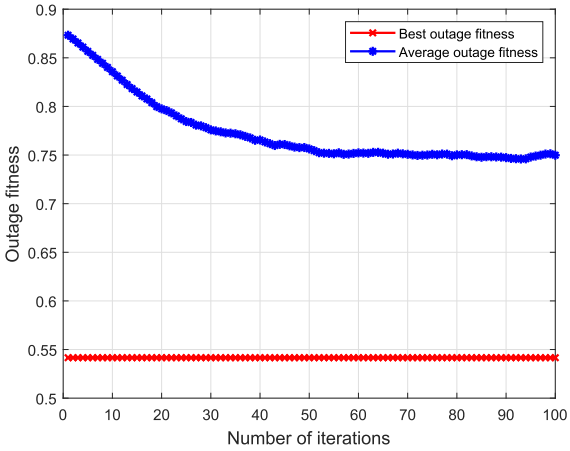

FIGURE 7. Outage fitness versus evolution iterations for SA-PSO-based resource allocation algorithm: $M = 3$, $N = 3$, $K = 3$, $I_p = 10$ dB.

algorithm can well approximate the optimal value by the exhaustive-searching-based algorithm. However, the computational complexity of the exhaustive-searching-based algorithm is much higher than that of the SA-PSO-based algorithm since exhaustive searching has to explore solutions in the two-dimensional continuous space given by constraints (11) and (12). In particular, for $I_p = 10$ dB, we present the WPT parameters setup optimized by the two algorithms. Obviously, both algorithms optimize the WPT power and the WPT time according to the system setup and the channel condition. However, for $K = 2$ and $K = 3$, the exhaustive-searching-based algorithm always employs the maximum WPT power to achieve the optimal outage performance, while the SA-PSO-based algorithm achieves similar outage performance with lower WPT power. For this case, we avoid unnecessary energy waste as the outage performance cannot be significantly enhanced with overmuch WPT.

Fig. 7 depicts how the SA-PSO-based resource allocation algorithm evolve with the number of evolution iterations increasing. Obviously, the best outage fitness always remains constant, indicating that the proposed algorithm obtains unique solution. In contrast, the average outage fitness first quickly decreases and then oscillates in a very limited region until the evolution iterations reach some value. Typically, after 50 evolution iterations, the outage fitness converges with little fluctuation. This indicates that the proposed SA-PSO-based resource allocation algorithm can quickly converge and has good stability.

VII. CONCLUSION

In this paper, we studied multi-hop CWPNs with multiple PBs underlying multiple PUs, wherein SUs harvest energy from the RF signals of multiple PBs and transmit concurrently with PUs under the interference power constraint. We derived both exact and asymptotic end-to-end outage probabilities, and obtained their closed-form expressions. Based on the outage analysis, we further formulated the outage minimization problem with respect to the WPT power and the WPT time. Due the complex expression of outage probability, we proposed the SA-PSO-based resource allocation algorithm to optimize the WPT parameters. By extensive simulations, we verified the correctness of the theoretical analysis and the effectiveness of the proposed algorithms. It is shown that the proposed SA-PSO-based resource allocation algorithm, with lower computational complexity, can efficiently optimize the WPT parameters according to the system setup and the channel condition.

APPENDIX A
PROOF OF PROPOSITION 1

Before the derivation, we first present some preliminary results on the cumulative distribution function (CDF) and the probability density function (PDF) of channel power gains. For notation convenience, we denote $X = \sum_{m=1}^{M} g_{m,k}$, $Y = \max_{n=1,\ldots,N} g_{k,n}$, and $Z = g_{k,k+1}$.

In Rayleigh fading channel, the power gain coefficient Z follows exponential distribution with rate parameter $\lambda_{D,k}$. Thus, the CDF and the PDF of exponential random variable Z are given by

$$F_Z(z) = 1 - \exp(-\lambda_{D,k} z), \tag{15}$$

$$f_Z(z) = \lambda_{D,k} \exp(-\lambda_{D,k} z). \tag{16}$$

As Y is the maximum of N independent exponential random variables, the CDF of Y is $F_Y(y) = \left(1 - \exp(-\lambda_{I,k} y)\right)^N$. By the binomial theorem, the CDF is rewritten as

$$F_Y(y) = 1 + \sum_{n=1}^{N} \binom{N}{n} (-1)^n \exp\left(-\lambda_{I,k} n y\right). \tag{17}$$

Then, the PDF of Y is given by

$$f_Y(y) = -\sum_{n=1}^{N} \binom{N}{n} (-1)^n n \lambda_{I,k} \exp\left(-\lambda_{I,k} n y\right). \tag{18}$$

As X is the summation of M independent exponential random variables, X follows Gamma distribution.

Hence, the CDF and the PDF of X are given by

$$F_X(x) = 1 - \sum_{m=0}^{M-1} \frac{(\lambda_{E,k}x)^m}{\Gamma(m+1)} \exp(-\lambda_{E,k}x), \tag{19}$$

$$f_X(x) = \frac{\lambda_{E,k}^M}{\Gamma(M)} x^{M-1} \exp(-\lambda_{E,k}x). \tag{20}$$

With CDFs and PDFs of X, Y and Z, we can derive $P_{\text{out},k}$ as follows:

$$\begin{aligned} P_{\text{out},k} &= \Pr\left(\frac{\min\left(K\eta\xi P_t X, \frac{I_p}{Y}\right) Z}{\sigma^2} \le \gamma_{\text{th}}\right) \\ &= \underbrace{\Pr\left(\frac{K\eta\xi P_t XZ}{\sigma^2} \le \gamma_{\text{th}}, K\eta\xi P_t X \le \frac{I_p}{Y}\right)}_{\mathcal{P}_1(\gamma_k)} \\ &\quad + \underbrace{\Pr\left(\frac{I_p Z}{\sigma^2 Y} \le \gamma_{\text{th}}, K\eta\xi P_t X > \frac{I_p}{Y}\right)}_{\mathcal{P}_2(\gamma_k)}. \end{aligned} \tag{21}$$

In the first summand $\mathcal{P}_1(\gamma_k)$, as the two terms both include X which is statistically independent of Z and Y, we can first calculate $\mathcal{P}_1(\gamma_k)$ conditioned on X. By employing (15) and (17), we have

$$\mathcal{P}_1(\gamma_k|X) = F_Z\left(\frac{\gamma_{\text{th}}\sigma^2}{K\eta\xi P_t X}\right) F_Y\left(\frac{I_p}{K\eta\xi P_t X}\right). \tag{22}$$

Then, with (20), by averaging $\mathcal{P}_1(\gamma_k|X)$ over the distribution of X and employing the equation (3.471.9) in [22] for the integral, we have

$$\begin{aligned} \mathcal{P}_1(\gamma_k) &= \int_0^\infty F_Z\left(\frac{\gamma_{\text{th}}\sigma^2}{K\eta\xi P_t x}\right) F_Y\left(\frac{I_p}{K\eta\xi P_t x}\right) f_x(x)dx \\ &= 1 - \frac{2}{\Gamma(M)}(\sqrt{\Delta_{1,k}})^M \mathcal{K}_M\left(2\sqrt{\Delta_{1,k}}\right) + \frac{2}{\Gamma(M)} \\ &\quad \times \sum_{n=1}^{N} \binom{N}{n} (-1)^n \left((\sqrt{n\Delta_{2,k}})^M \mathcal{K}_M\left(2\sqrt{n\Delta_{2,k}}\right)\right. \\ &\quad \left. - (\sqrt{\Delta_{1,k}+n\Delta_{2,k}})^M \mathcal{K}_M\left(2\sqrt{\Delta_{1,k}+n\Delta_{2,k}}\right)\right). \end{aligned} \tag{23}$$

Similarly, the two terms in the second summand $\mathcal{P}_2(\gamma_k)$ both include Y that is statistically independent of Z and X. Thus, by employing (15) and (19), we can calculate $\mathcal{P}_2(\gamma_k)$ conditioned on Y as

$$\mathcal{P}_2(\gamma_k|Y) = F_Z\left(\frac{\gamma_{\text{th}}\sigma^2 Y}{I_p}\right)\left(1 - F_X\left(\frac{I_p}{K\eta\xi P_t Y}\right)\right). \tag{24}$$

Then, with (18), the unconditional CDF marginalized out Y is given by

$$\begin{aligned} &\mathcal{P}_2(\gamma_k) \\ &= \int_0^\infty F_Z\left(\frac{\gamma_{\text{th}}\sigma^2 y}{I_p}\right)\left(1 - F_X\left(\frac{I_p}{K\eta\xi P_t y}\right)\right) f_Y(y)dy \\ &= -2\sum_{n=1}^{N} \binom{N}{n} (-1)^n \sum_{m=0}^{M-1} \frac{n\Delta_{2,k}}{\Gamma(m+1)} \\ &\quad \times \left((\sqrt{n\Delta_{2,k}})^{m-1} \mathcal{K}_{1-m}\left(2\sqrt{n\Delta_{2,k}}\right)\right. \\ &\quad \left. - (\sqrt{\Delta_{1,k}+n\Delta_{2,k}})^{m-1} \mathcal{K}_{1-m}\left(2\sqrt{\Delta_{1,k}+n\Delta_{2,k}}\right)\right), \end{aligned} \tag{25}$$

where the equation (3.471.9) in [22] is also utilized for the integral during the derivation.

Finally, by substituting (23) and (25) into (21), we obtain (7) and complete the proof.

APPENDIX B
PROOF OF PROPOSITION 2

When $P_t \ll I_p$, $P_k \approx K\xi\eta P_t \sum_{m=1}^{M} g_{m,k}$ according to (3). Thus, by employing (15) and (20), we have

$$\begin{aligned} P_{\text{out},k}^{\text{slack}} &\overset{P_t \ll I_p}{=} \Pr\left(\frac{K\eta\xi P_t XZ}{\sigma^2} \le \gamma_{\text{th}}\right) \\ &= \int_0^\infty F_Z\left(\frac{\gamma_{\text{th}}\sigma^2}{K\eta\xi P_t x}\right) f_X(x)dx \\ &= 1 - \frac{2}{\Gamma(M)}(\sqrt{\Delta_{1,k}})^M \mathcal{K}_M\left(2\sqrt{\Delta_{1,k}}\right), \end{aligned} \tag{26}$$

wherein the equation (3.471.9) in [22] is utilized for the integral.

Then, by substituting (26) into (6), we have (8) and complete the proof.

APPENDIX C
PROOF OF PROPOSITION 3

When $P_t \gg I_p$, $P_k \approx \frac{I_p}{\max\limits_{n=1,\ldots,N} g_{n,k}}$ according to (3). Thus, by employing (15) and (18), we have

$$\begin{aligned} P_{\text{out},k}^{\text{strict}} &\overset{P_t \gg I_p}{=} \Pr\left(\frac{I_p Z}{\sigma^2 Y} \le \gamma_{\text{th}}\right) \\ &= \int_0^\infty F_Z\left(\frac{I_p Z}{\sigma^2 Y} \le \gamma_{\text{th}}\right) f_Y(y)dy \\ &= 1 + \sum_{n=1}^{N} \binom{N}{n} (-1)^n \frac{n\Delta_{2,k}}{\Delta_{1,k}+n\Delta_{2,k}}. \end{aligned} \tag{27}$$

Then, by substituting (27) into (6), we have (9) and complete the proof.

REFERENCES

[1] X. Huang, T. Han, and N. Ansari, "On green-energy-powered cognitive radio networks," *IEEE Commun. Surveys Tuts.*, vol. 17, no. 2, pp. 827–842, 2nd Quart., 2015.
[2] K. Huang and V. K. N. Lau, "Enabling wireless power transfer in cellular networks: Architecture, modeling and deployment," *IEEE Trans. Wireless Commun.*, vol. 13, no. 2, pp. 902–912, Feb. 2014.
[3] K. Huang and X. Zhou, "Cutting the last wires for mobile communications by microwave power transfer," *IEEE Commun. Mag.*, vol. 53, no. 6, pp. 86–93, Jun. 2015.
[4] A. Goldsmith, S. A. Jafar, I. Maric, and S. Srinivasa, "Breaking spectrum gridlock with cognitive radios: An information theoretic perspective," *Proc. IEEE*, vol. 97, no. 5, pp. 894–914, Apr. 2009.

[5] S. Lee, R. Zhang, and K. Huang, "Opportunistic wireless energy harvesting in cognitive radio networks," *IEEE Trans. Wireless Commun.*, vol. 12, no. 9, pp. 4788–4799, Sep. 2013.
[6] A. H. Sakr and E. Hossain, "Cognitive and energy harvesting-based D2D communication in cellular networks: Stochastic geometry modeling and analysis," *IEEE Trans. Commun.*, vol. 63, no. 5, pp. 1867–1880, May 2015.
[7] D. T. Hoang, D. Niyato, P. Wang, and D. I. Kim, "Opportunistic channel access and RF energy harvesting in cognitive radio networks," *IEEE J. Sel. Areas Commun.*, vol. 32, no. 11, pp. 2039–2052, Nov. 2014.
[8] H. S. Lee, M. E. Ahmed, and D. I. Kim, "Optimal spectrum sensing policy in RF-powered cognitive radio networks," *IEEE Trans. Veh. Technol.*, vol. 67, no. 10, pp. 9557–9570, Oct. 2018.
[9] Z. Wang, Z. Chen, B. Xia, L. Luo, and J. Zhou, "Cognitive relay networks with energy harvesting and information transfer: Design, analysis, and optimization," *IEEE Trans. Wireless Commun.*, vol. 15, no. 4, pp. 2562–2576, Apr. 2016.
[10] Y. Wang, W. Lin, R. Sun, and Y. Huo, "Optimization of relay selection and ergodic capacity in cognitive radio sensor networks with wireless energy harvesting," *Pervas. Mobile Comput.*, vol. 22, pp. 33–45, Sep. 2015.
[11] S. Lee and R. Zhang, "Cognitive wireless powered network: Spectrum sharing models and throughput maximization," *IEEE Trans. Cognit. Commun. Netw.*, vol. 1, no. 3, pp. 335–346, Mar. 2015.
[12] S. S. Kalamkar, J. P. Jeyaraj, A. Banerjee, and K. Rajawat, "Resource allocation and fairness in wireless powered cooperative cognitive radio networks," *IEEE Trans. Commun.*, vol. 64, no. 8, pp. 3246–3261, Aug. 2016.
[13] S. Yin, Z. Qu, Z. Wang, and L. Li, "Energy-efficient cooperation in cognitive wireless powered networks," *IEEE Commun. Lett.*, vol. 21, no. 1, pp. 128–131, Jan. 2017.
[14] W. Lu *et al.*, "Joint resource allocation for wireless energy harvesting enabled cognitive sensor networks," *IEEE Access*, vol. 6, pp. 22480–22488, May 2018.
[15] C. Xu, M. Zheng, W. Liang, H. Yu, and Y.-C. Liang, "End-to-end throughput maximization for underlay multi-hop cognitive radio networks with RF energy harvesting," *IEEE Trans. Wireless Commun.*, vol. 16, no. 6, pp. 3561–3572, Jun. 2017.
[16] C. Xu, W. Liang, and H. Yu, "Green-energy-powered cognitive radio networks: Joint time and power allocation," *Trans. Embedded Comput. Syst.*, vol. 17, no. 1, pp. 13:1–13:18, Jan. 2018.
[17] Z. Yang, Z. Ding, P. Fan, and G. K. Karagiannidis, "Outage performance of cognitive relay networks with wireless information and power transfer," *IEEE Trans. Veh. Technol.*, vol. 65, no. 5, pp. 3828–3833, May 2016.
[18] C. Xu, M. Zheng, W. Liang, H. Yu, and Y.-C. Liang, "Outage performance of underlay multihop cognitive relay networks with energy harvesting," *IEEE Commun. Lett.*, vol. 20, no. 6, pp. 1148–1151, Jun. 2016.
[19] R. Zhang and C. K. Ho, "MIMO broadcasting for simultaneous wireless information and power transfer," *IEEE Trans. Wireless Commun.*, vol. 12, no. 5, pp. 1989–2001, May 2013.
[20] T. Q. Duong, P. L. Yeoh, V. N. Q. Bao, M. Elkashlan, and N. Yang, "Cognitive relay networks with multiple primary transceivers under spectrum-sharing," *IEEE Signal Process. Lett.*, vol. 19, no. 11, pp. 741–744, Nov. 2012.
[21] C. Xu, M. Zheng, W. Liang, and H. Yu, "Joint spatial-temporal access scheme for multihop cognitive relay networks over Nakagami-*m* fading," *Wireless Pers. Commun.*, vol. 95, no. 3, pp. 3097–3117, Aug. 2017.
[22] I. S. Gradshteyn and I. M. Ryzhik, *Table of Integrals, Series, and Products*, 8th ed. San Diego, CA, USA: Academic, 2014.
[23] M. Clerc and J. Kennedy, "The particle swarm—Explosion, stability, and convergence in a multidimensional complex space," *IEEE Trans. Evol. Comput.*, vol. 6, no. 1, pp. 58–73, Feb. 2002.

CHI XU (M'18) received the Ph.D. degree from University of Chinese Academy of Sciences, China, in 2017. He has been with Shenyang Institute of Automation, Chinese Academy of Sciences, China, since 2013, where he is currently an Assistant Professor. His research interests include cognitive radio networks, wireless sensor networks, industrial wireless networks, and 5G URLLC. He is a member of China Computer Federation, and Chinese Association of Automation. He also serves as the 3GPP standardization delegate in the Technical Specification Group for Radio Access Network.

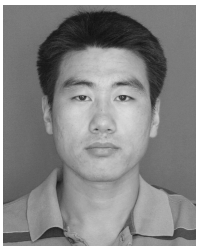

CHANGQING XIA received the Ph.D. degree from Northeastern University, China, in 2015. He is currently an Assistant Professor with Shenyang Institute of Automation, Chinese Academy of Sciences. His research interests include wireless sensor networks and real-time systems, especially the real-time scheduling algorithms and smart energy systems.

CHUNHE SONG received the Ph.D. degree from Northeastern University, China, in 2012. From 2012 to 2015, he completed his post-doctoral research at University of Waterloo, Canada, and University of Ontario Institute of Technology, Canada. In 2015, he was a Senior System Scientist at CIM Technology Inc., Canada. Since 2016, he has been a Professor with Shenyang Institute of Automation, Chinese Academy of Sciences, China. His research interests include wearable computing, image processing, and wireless communication.

PENG ZENG received the Ph.D. degree from Shenyang Institute of Automation, Chinese Academy of Sciences, China, in 2005. He has been a Professor with Shenyang Institute of Automation, Chinese Academy of Sciences, China, since 2007. He is an Expert Member of the IEC/TC65/WG16, a member of the standards committee of SP100, and a member of the Wireless WG of FieldBus Foundation. He also serves as the Chair of Edge Computing Technical Committee, Chinese Association of Automation. His research interests include wireless sensor networks and industrial wireless communications.

HAIBIN YU received the Ph.D. degree from Northeastern University, China, in 1997. He has been a Professor with Shenyang Institute of Automation, Chinese Academy of Sciences, China, since 1997, where he is serving as the Director. He has published two books, authored or co-authored over 200 papers, and held over 50 patents. His research interests include wireless sensor networks, industrial communication and networked control, industrial automation, and intelligent manufacturing. He and his research team have proposed the WIA-PA and WIA-FA standards which are specified as IEC 62601 and IEC 62948, respectively. He was elected as an ISA Fellow for his contributions in fieldbus technologies in 2011. He serves as the Chair of IEC ACART, the Vice-Chair of Chinese Association of Automation, the Chair of China National Technical Committee for Industrial Process Measurement Control and Automation Standardization, and the Associate Editor-in-Chief of the Chinese Journal *Information and Control*.